

## Using Sweep Frequency Response Analysis and Dissolved Gas Analysis in Diagnosing of Power Transformer

Hoang Minh Vu Nguyen 

University of Architecture Ho Chi Minh City, Vietnam

\*Corresponding author. Email: [vu.nguyenhoangminh@uah.edu.vn](mailto:vu.nguyenhoangminh@uah.edu.vn)

### ARTICLE INFO

Received: 12/08/2025  
Revised: 11/09/2025  
Accepted: 19/09/2025  
Published online: 06/03/2026

### KEYWORDS

Power Transformer;  
Sweep Frequency Response Analysis (SFRA);  
Dissolved Gas Analysis (DGA);  
Diagnostic;  
Diagnosing of Power Transformer.

### ABSTRACT

This article presents two diagnostic techniques for assessing the mechanical and electrical condition of oil-immersed power transformers: sweep frequency response analysis (SFRA) and dissolved gas analysis (DGA). The SFRA method detects potential mechanical faults in transformer windings by applying the correlation coefficient ( $R_{xy}$ ). For a 63 MVA, 115/23/11 kV transformer, experimental results show that the winding is considered normal when  $RLF \geq 2.0$ ,  $RMF \geq 1.0$ , and  $RHF \geq 0.6$ , whereas  $RLF < 0.6$  indicates severe deformation. In contrast, the DGA method identifies internal faults such as partial discharge, low-energy and high-energy discharges, and thermal faults by analyzing gas concentrations in the insulating oil. For a 20 MVA, 110/22 kV transformer, measured gas concentrations ( $\mu\text{l/l}$ , ppm) include  $\text{H}_2$  (0.00),  $\text{CH}_4$  (40.43),  $\text{C}_2\text{H}_6$  (18.24),  $\text{C}_2\text{H}_4$  (20.92),  $\text{C}_2\text{H}_2$  (0.00),  $\text{CO}_2$  (8932.66), and  $\text{CO}$  (2131.18), corresponding to a “thermal fault below 300°C.” Both diagnostic methods are integrated into user-friendly MATLAB-based tools to support testing centers in Vietnam. The combination of SFRA and DGA enhances diagnostic accuracy, enables timely maintenance decisions, and contributes to improving the reliability of power supply systems.

Doi: <https://doi.org/10.54644/jte.2026.1978>

Copyright © JTE. This is an open access article distributed under the terms and conditions of the [Creative Commons Attribution-NonCommercial 4.0 International License](https://creativecommons.org/licenses/by-nc/4.0/) which permits unrestricted use, distribution, and reproduction in any medium for non-commercial purpose, provided the original work is properly cited.

### 1. Introduction

In operating and maintaining power transformers (PTs), diagnosing mechanical and electrical faults is essential to prevent failures and power interruptions. Undetected winding deformation or core displacement can cause dielectric or thermal damage, leading to costly repairs or replacement. Therefore, mechanical integrity should be checked after transportation, periodically, and after short circuits. The Sweep Frequency Response Analysis (SFRA) technique is a powerful tool for detecting minor displacements in windings and magnetic circuits, with ongoing research [1]–[10]. In [11], failures were analyzed using Transformer Turns Ratio (TTR) and SFRA, showing a linear correlation and confirming TTR’s ability to detect short-circuit faults. However, TTR cannot identify discharge faults or internal damage. In [12], SFRA was used for temporary condition checks by comparing healthy and faulty responses, with discussion on analysis methods and limitations. In [13], transformer parameters were estimated from SFRA data using an RLC model with mutual inductance, achieving good agreement between the simulated and measured responses; however, the approach was limited to single-phase transformers.

In [14], an improved SFRA-based fault localization method applied regression analysis on data from 70 oil-immersed PTs of various designs, capacities, and manufacturers. In [15], climate, oil thermal parameters, and photovoltaic (PV) systems were studied for their effect on thermal performance, focusing on hottest-spot temperature (HST) and top oil temperature (TOT) under ONAN cooling, without addressing ONAF types or mechanical/electrical discharge faults. The work in [16] used SFRA with statistical parameters to detect and locate short-circuit faults, deriving Min–Max (MM) ratios from healthy and faulty measurements, but considered no other fault types. In [17], partial discharge detection was achieved using multi-wall carbon nanotubes (MWNT) for online monitoring, though mechanical and short-circuit detection were not covered.

In [18], SFRA was applied to evaluate insulation degradation by analyzing winding capacitance changes from peak frequency shifts; negative changes indicated deterioration. The authors in [19] diagnosed voltage regulator faults using SFRA with multiple configurations and correlation coefficient (CC) analysis, showing sensitivity to tap changer coking (low-frequency magnitude drop at 20 Hz–2 kHz) and pitting (shift to higher frequencies). During PT operation, oil decomposition under heat and high electromagnetic fields produces gases such as H<sub>2</sub>, CH<sub>4</sub>, and C<sub>2</sub>H<sub>6</sub>. Measuring gas content in insulating oil aids early diagnosis. Dissolved Gas Analysis (DGA) with gas generation monitoring detects electrical faults, supporting safe, efficient operation, with ongoing research [20]–[27]. In [28], DGA diagnosed partial discharges, low/high-energy discharges, and low/medium/high thermal faults using dissolved gas concentrations, applying techniques like the new approach, conditional probability, and Duval methods. However, [28] addressed only electrical faults. Since PT faults can be mechanical or electrical, research should address both diagnostics and develop tools to support effective fault identification.

## 2. Sweep frequency response analysis (SFRA) technique

### 2.1. Principle of SFRA

The Sweep Frequency Response Analysis (SFRA) technique [7]–[10] measures the transformer’s impedance-to-conductance ratio across a wide frequency range. This amplitude, expressed as a transfer function, serves as the PT’s “fingerprint,” and deviations from the baseline indicate abnormalities in the coil or magnetic circuit. The SFRA wiring diagram and phase frequency response characteristics (amplitude and phase angle) are shown in Figure 1 and Figure 2.

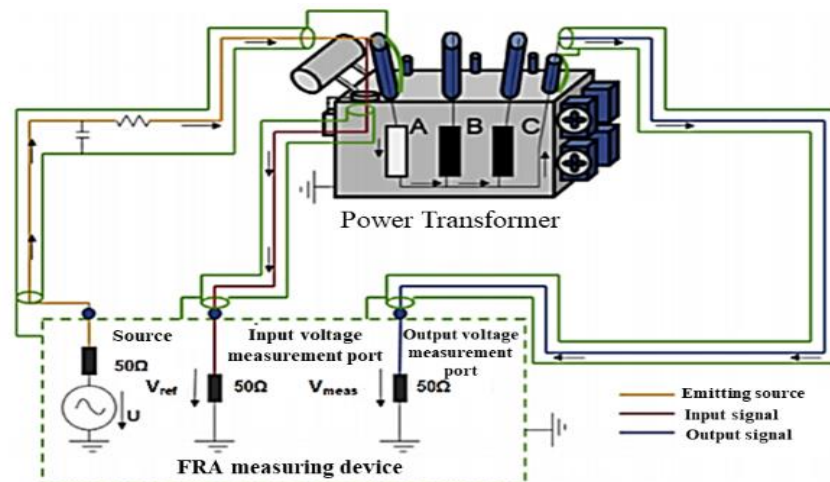


**Figure 1.** SFRA measurement wiring diagram.

For SFRA measurement, a low-voltage sinusoidal signal (1–10 Vrms) with variable frequency (typically 20 Hz–2 MHz, depending on coil structure and measurement system) is applied. The amplitude and phase angle of the frequency response are calculated using equations (1) and (2):

$$\text{Amplitude (dB): } 20 \log_{10}(|V_{meas}|/|V_{ref}|) \quad (1)$$

$$\text{Phase angle (}^\circ\text{): } \text{pha}\{V_{meas}\} - \text{pha}\{V_{ref}\} \quad (2)$$

SFRA is mainly applied to detect mechanical faults, including winding deformation, displacement, and core movement. This makes SFRA particularly suitable for identifying structural problems that affect the mechanical integrity of transformers.

### 2.2. Scope and conditions of application of SFRA

SFRA is commonly applied to transformers above 6 kV and should be used in the following cases, based on international experience:

These include all new PTs to obtain initial data (the fingerprint), as part of routine electrical tests, and after reinstalling the PT. SFRA is also recommended in cases of long-term short circuits downstream

of the transformer, after repairing the tap changer, and following vacuum treatment, oil filtration, or oil regeneration. Furthermore, the method should be applied after any faults occur in the PT. The application of SFRA measurements for PTs is regulated under the IEC60076-18 standard [29].

### 2.3. The SFRA's ability to detect faults

SFRA can detect winding deformation, displacement, short and open circuits, loose core components, coil collapse, core grounding damage, and tap changer faults. It can also identify faults at the core joints, localized coil collapse, damage to the core grounding, and movement of the core. Additionally, SFRA is effective in detecting issues related to the connection between the windings and the porcelain input, as well as the on-load tap changer. It is noteworthy that the influence of mechanical deformations on SFRA characteristics may vary depending on the structure and design of the PT.

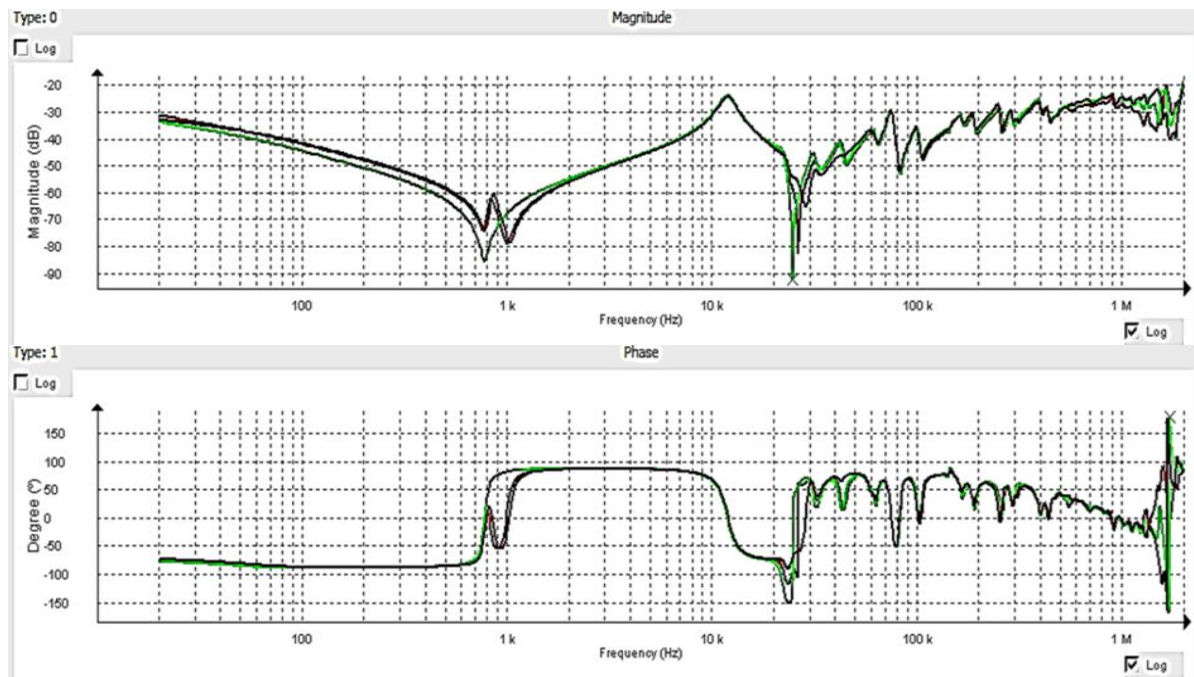


**Figure 2.** Phase frequency response characteristic (amplitude, phase angle), 63 MVA, 110/22 kV, YNyn0d11.

### 2.4. Diagnosis of PT quality using SFRA

#### 2.4.1. Qualitative analysis method

Analyze the differences in the SFRA characteristics [29], [30]. There are 4 basic SFRA measurement schemes presented in Figure 3:

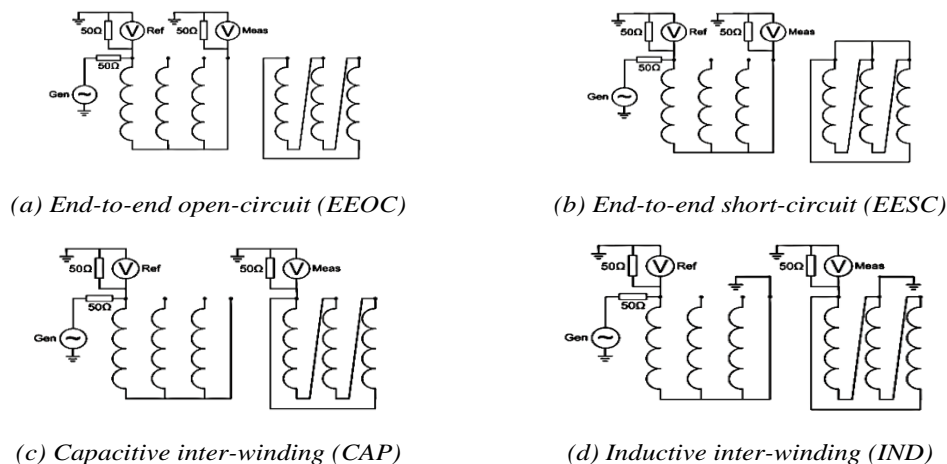


**Figure 3.** Four basic SFRA measurement schemes.

(a) Figure 4 show the LV winding buckling and its frequency response.

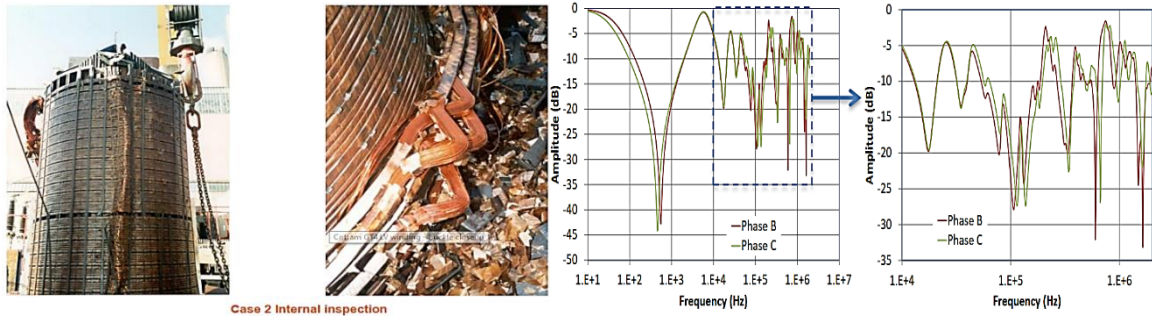


**Figure 4.** LV winding Buckling and SFRA frequency characteristics.

(b) Figure 5 and Figure 6 illustrate twisting and loosening of the clamping fault and its frequency response.



**Figure 5.** Twisting and loosening of the clamping fault.

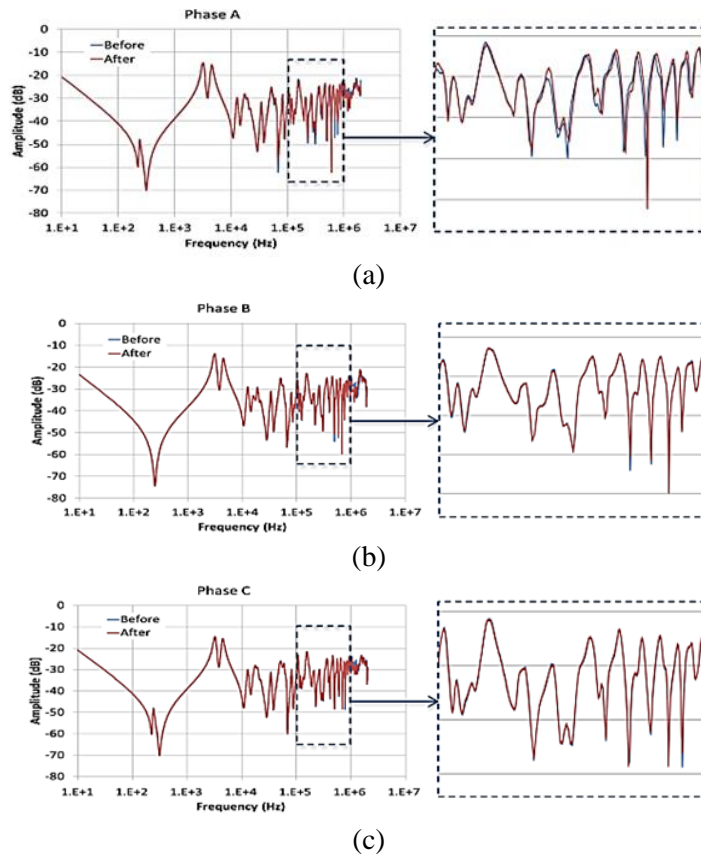


**Figure 6.** SFRA frequency characteristics curves in the case of twisted and loose PT winding.

(c) Figure 7 and Figure 8 present axial deformation of the LV winding and its frequency response.



Case 6 Internal inspection

**Figure 7. Winding axial deformation problem.**

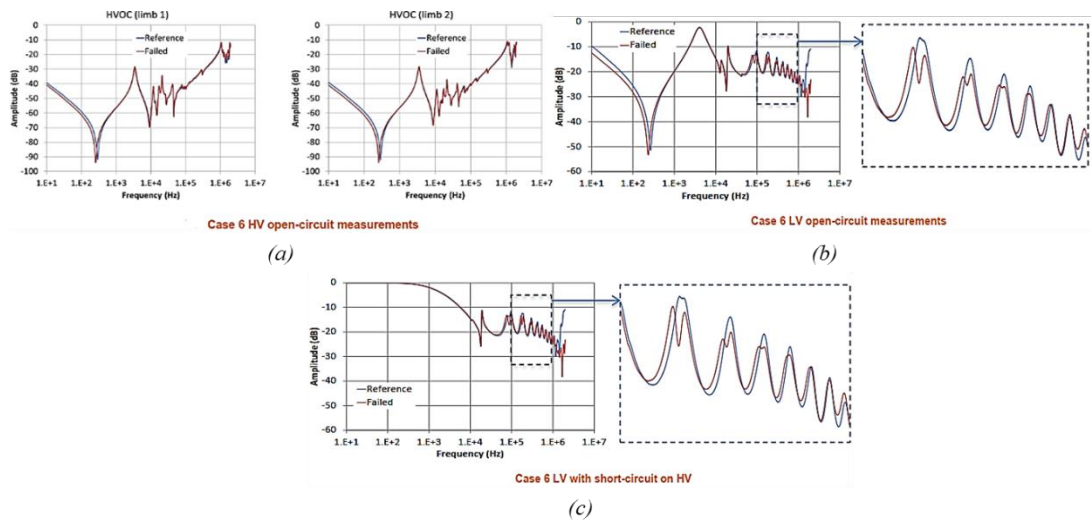


**Figure 8. SFRA frequency characteristics in the case of winding axial deformation.**

(d) Figure 9 and Figure 10 show a short circuit inside the winding and the corresponding frequency response.



**Figure 9. Short circuit inside the winding.**

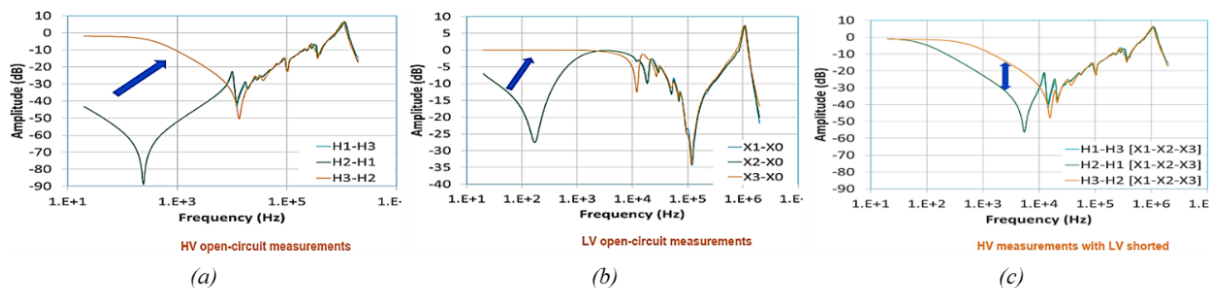


**Figure 10. SFRA frequency characteristics in the case of a short circuit inside the winding [3].**

2.4.2. Quantitative analysis method: using the correlation factor through SFRA measurement

(a) The Chinese standard DL/T 911 – 2004 [31] is the only international standard that addresses how to quantitatively compare two frequency responses by calculating the correlation factor - R between two signals in three frequency ranges: Low frequency: from 1 kHz to 100 kHz, Medium frequency: from 100 kHz to 600 kHz, High frequency: from 600 kHz to 1 MHz.

Suppose that there are two results obtained, with N amplitude values corresponding to N frequencies, denoted as X(k), Y(k), where k= 0, 1... N-1. The correlation factor R can then be calculated through the following equations from (3) to (7):

Calculate the standard variance of these two sequences according to equations (3) and (4):

$$D_x = \frac{1}{N} \sum_{k=0}^{N-1} \left[ X(k) - \frac{1}{N} \sum_{k=0}^{N-1} X(k) \right]^2 \quad (3)$$

$$D_y = \frac{1}{N} \sum_{k=0}^{N-1} \left[ Y(k) - \frac{1}{N} \sum_{k=0}^{N-1} Y(k) \right]^2 \quad (4)$$

Calculate the covariance of these two sequences according to equation (5):

$$C_{xy} = \frac{1}{N} \sum_{k=0}^{N-1} \left[ X(k) - \frac{1}{N} \sum_{k=0}^{N-1} X(k) \right] \times \left[ Y(k) - \frac{1}{N} \sum_{k=0}^{N-1} Y(k) \right] \quad (5)$$

Calculate the normalization covariance factor of these two sequences according to equation (6):

$$LR_{xy} = C_{xy} / \sqrt{D_x D_y} \quad (6)$$

Because the LR<sub>xy</sub> value is always in the range [-1,1] and usually has a very small value, it can be converted to the quantity R<sub>xy</sub> for easy comparison.

Calculate the correlation factor according to equation (7):

$$R_{xy} = \begin{cases} 10 & 1 - LR_{xy} < 10^{-10} \\ -\lg(1 - LR_{xy}) & \text{others} \end{cases} \quad (7)$$

From there, the correlation factor R<sub>xy</sub> quantifies the difference between two signals. According to the DT/T911–2004 standard, the calculated values are assessed using the criteria in Table 1.

(b) Diagnosis of potential faults according to the SFRA method for a typical PT.

The quantitative diagnosis of potential transformer faults using the SFRA method is presented in Table 1.

**Table 1.** Quantitative assessment of transformer winding mechanical fault diagnosis.

Winding Deformation degree	Winding Deformation degree
Severe Deformation	R <sub>LF</sub> < 0.6
Obvious Deformation	1.0 > R <sub>LF</sub> ≥ 0.6 or R <sub>MF</sub> < 0.6
Slight Deformation	2.0 > R <sub>LF</sub> ≥ 1.0 or 0.6 ≤ R <sub>MF</sub> < 1.0
Normal Winding	R <sub>LF</sub> ≥ 2.0, R <sub>MF</sub> ≥ 1.0 and R <sub>HF</sub> ≥ 0.6

Note: R<sub>LF</sub> represents the correlation factor when the curve is in low frequency band (1 kHz~100 kHz);  
R<sub>MF</sub> represents the correlation factor when the curve is in medium frequency band (100 kHz~600 kHz);  
R<sub>HF</sub> represents the correlation factor when the curve is in high frequency band (600 kHz~1000 kHz).

Analyzing the SFRA characteristics of the Phan Thiet 63 MVA, 110/22 kV, YNyn0d11 Transformer is shown in Figure 11 and the correlation factors are presented in Table 2.

**Table 2.** Correlation coefficient determined from the SFRA characteristics of the Phan Thiet 63 MVA, 110/22 kV transformer.

Phase	R <sub>LF</sub>	R <sub>MF</sub>	R <sub>HF</sub>
[A-N (open)]-[B-N (open)]	1.25	1.92	1.09
[B-N (open)]-[C-N (open)]	1.38	1.55	1.08
[C-N (open)]-[A-N (open)]	1.02	1.87	1.36

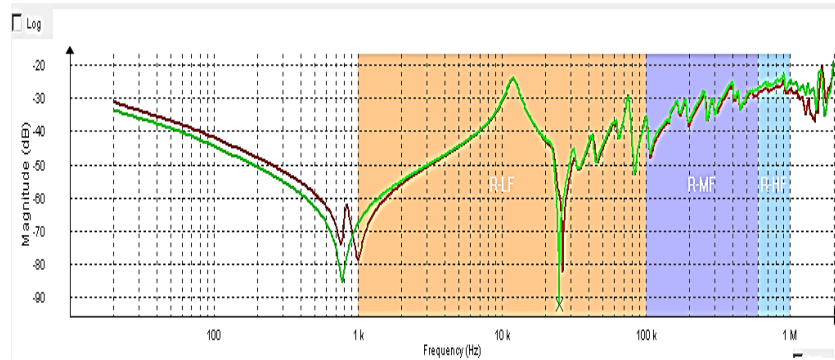


**Figure 11.** SFRA frequency characteristics in the case of short circuits inside the winding.

To support users in making quick decisions regarding the diagnosis of transformer faults, the MATLAB-based SFRA-TRAFADI program was developed using correlation factors RLF, RMF, and RHF. Its interface is shown in Figure 12a.

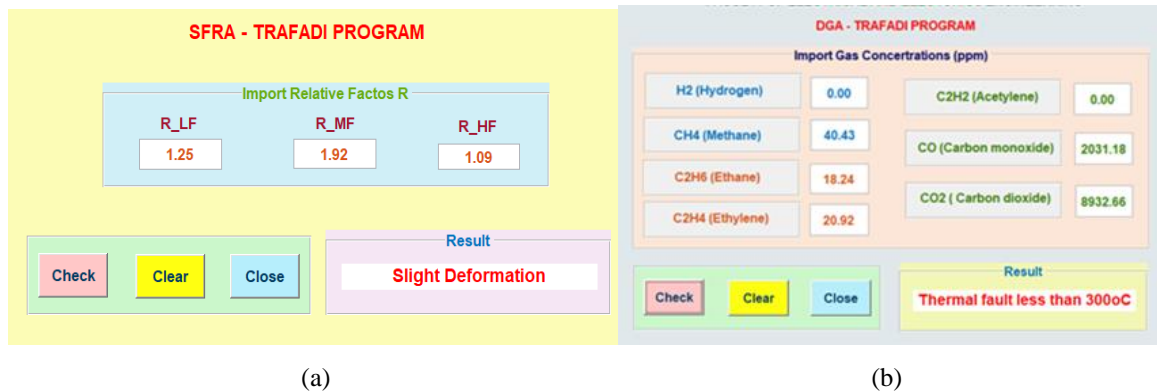


**Figure 12.** SFRA – TRAFADI and DGA – TRAFADI program interface.

This interface is not only a guide in Matlab but also demonstrates the practical implementation of the SFRA–TRAFADI program. By providing a user-friendly environment, the tool allows engineers at testing centers to apply SFRA diagnostics directly, supporting quick and accurate decision-making without requiring complex programming knowledge.

The correlation data determined from the SFRA characteristics and the results of diagnosing potential faults of the Phan Thiet 63 MVA, 110/22 kV transformer using the SFRA-TRAFADI software, compared with the diagnostic results from the Southern Vietnam Power Testing Company (EVNSPC), are presented in Table 3 and Table 4, respectively.

**Table 3.** Conclusion of Diagnosis of Transformer Phan Thiet 63 MVA, 110/22 kV Condition.

Phases	Results
[A-N (open)]-[B-N (open)]	Slight deformation
[B-N (open)]-[C-N (open)]	
[C-N (open)]-[A-N (open)]	

Similarly, the correlation coefficients determined from the SFRA characteristics of the Ngai Giao 40 MVA, 110/22 kV transformer and the results of diagnosing potential faults using the SFRA-TRAFADI software, compared with the diagnostic results from the Southern Vietnam Power Testing Company (EVNSPC), are presented in Table 4 and Table 5.

**Table 4.** Correlation Coefficients Determined from the SFRA Characteristics of the Ngai Giao 40 MVA, 110/22 kV Transformer.

Phases	$R_{LF}$	$R_{MF}$	$R_{HF}$
[A-N (open)]-[BN (open)]	2.01	2.58	2.52
[B-N (open)]-[C-N (open)]	2.3	2.25	1.86
[C-N (open)]-[A-N (open)]	2.03	2.6	1.85

**Table 5.** Conclusion of Diagnosis of Ngai Giao 40 MVA, 110/22 kV Transformer Condition.

Phases	SFRA-TRAFADI	EVNSPC
[A-N (open)]-[B-N (open)]	Normal	Normal
[B-N (open)]-[C-N (open)]	-	-
[C-N (open)]-[A-N (open)]	-	-

### 3. Dissolved gas analysis techniques (DGA) in transformer oil

#### 3.1. Principle of DGA

Dissolved Gas Analysis (DGA) [21], [22], [24], [27] diagnoses thermal and electrical faults in transformers by measuring the concentration of dissolved gases in insulating oil or extracted gas samples. This technique has been standardized according to the international standards IEEE C57.104 [32] and IEC 60599 [33]. In contrast, DGA is primarily used to diagnose electrical and thermal faults, such as partial discharges, low-energy and high-energy discharges, and overheating at different temperature levels. This enables early detection of insulation and thermal degradation inside the transformer.

#### 3.2. DGA assessment methods

- Main gas method:  $C_2H_4$ ; CO;  $H_2$ ;  $C_2H_2$ .
- Roger ratio method [30], [31] uses the ratios:  $CH_4/H_2$ ;  $C_2H_4/C_2H_6$  and  $C_2H_2/C_2H_4$ .

The gas generation diagram according to PT temperature is presented in Figure 13.

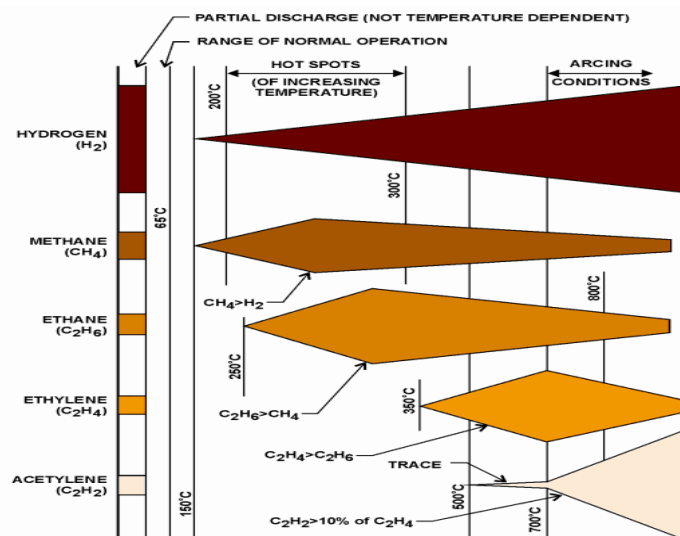


**Figure 13.** Diagram of gas generation according to temperature in PT oil.

### 3.3. Fault classification

Table 6 presents the fault of classification according to the IEE C57.104 standard [32]. Table 7 provides the fault classification based on temperature in oil of PT in accordance with the IEC 60559 standard.

**Table 6.** Fault classification according to temperature in oil of PT according to IEEE C57.104 standard.

Thermal fault: $150^{\circ}\text{C} < t \leq 500^{\circ}\text{C}$	Between $150^{\circ}\text{C}$ and $500^{\circ}\text{C}$ , oil decomposition produces mainly hydrogen and methane, with smaller amounts of ethylene and ethane.
Discharges of low energy	Low-energy discharges generate hydrogen, methane, and traces of acetylene.
Discharges of high energy $t \geq 700^{\circ}\text{C}$	High-energy discharges ( $700\text{--}1800^{\circ}\text{C}$ ) significantly increase acetylene content.

**Table 7.** Fault classification according to temperature in oil of PT according to the IEC 60559 standard.

Case	Characteristic fault
PD	Partial discharges
D1	Discharges of low energy
D2	Discharges of high energy
T1	Thermal fault, $t < 300^{\circ}\text{C}$
T2	Thermal fault, $300^{\circ}\text{C} < t < 700^{\circ}\text{C}$
T3	Thermal fault, $t > 700^{\circ}\text{C}$

### 3.4. The measurement of DGA in insulating oils

Dissolved Gas Analysis (DGA) measurements were performed using an Agilent 7890A Gas Chromatograph (Agilent Technologies) in accordance with the ASTM D3612C standard method, with a detection limit of 1 ppm. The detectable gases included  $\text{O}_2$ ,  $\text{N}_2$ ,  $\text{H}_2$ ,  $\text{CO}$ ,  $\text{CO}_2$ ,  $\text{CH}_4$ ,  $\text{C}_2\text{H}_6$ ,  $\text{C}_2\text{H}_4$ ,  $\text{C}_2\text{H}_2$ ,  $\text{C}_3\text{H}_6$ , and  $\text{C}_4\text{H}_8$ . The Agilent 7890A chromatograph system was employed to quantify the concentration of dissolved gases in transformer oil samples. DGA method is widely used in transformer fault diagnosis.

Table 8 shows the concentrations of individual gases and total dissolved gas.

**Table 8.** Single gas concentration in oil ( $\mu\text{l/l}$ , ppm), TCG: total combustion gas concentration (ppm) of Transformer T1.

$\text{CO}_2$	$\text{C}_2\text{H}_4$	$\text{C}_2\text{H}_2$	$\text{C}_2\text{H}_6$	$\text{H}_2$
8932.66	20.92	0.00	18.24	0.00
$\text{O}_2$	$\text{N}_2$	$\text{CH}_4$	$\text{CO}$	TCG
7805.28	53315.2	40.43	2131.18	2118

- According to the concentration of flammable gas in the oil

Table 9 presents the threshold for flammable gas concentration (single) in oil ( $\mu\text{l/l}$ , ppm) according to IEC 60599 [33].

**Table 9.** Threshold for flammable gas concentration (single) in oil ( $\mu\text{l/l}$ , ppm) according to IEC 60599.

$\text{C}_2\text{H}_2$	$\text{H}_2$	$\text{CH}_4$
1	100	120
$\text{C}_2\text{H}_6$	$\text{CO}$	$\text{C}_2\text{H}_4$
65	350	50

- According to the Roger combustion gas ratio [32], [33], Table 10 presents threshold of flammable gas in oil according to IEEE C57.104.

**Table 10.** Threshold of flammable gas in oil according to IEEE C57.104.

Faults	R1	R2	R5
	CH <sub>4</sub> /H <sub>2</sub>	C <sub>2</sub> H <sub>2</sub> /C <sub>2</sub> H <sub>4</sub>	C <sub>2</sub> H <sub>4</sub> /C <sub>2</sub> H <sub>6</sub>
No fault	> 0.1 to < 1.0	< 1.0	< 1.0
PD (corona partial discharges)	< 1.0	< 1.0	< 1.0
Arc of high energy	0.1 – 1.0	0.1 – 0.3	> 3.0
Low temperature	> 0.1 to < 1.0	< 1.0	1 - 3
Temperatures below 700°C	> 1.0	< 1.0	1 - 3
Temperatures above 700°C	> 1.0	< 1.0	> 3.0

Table 11 presents threshold of flammable gas in oil according to IEC 60599.

**Table 11.** Threshold of flammable gas in oil according to IEC 60599.

Case	Characteristic fault	C <sub>2</sub> H <sub>2</sub> /C <sub>2</sub> H <sub>4</sub>	CH <sub>4</sub> /H <sub>2</sub>	C <sub>2</sub> H <sub>4</sub> /C <sub>2</sub> H <sub>6</sub>
PD	Partial discharges	-	< 0.1	< 0.2
D1	Discharges of low energy	>1	0.1 – 0.5	> 1
D2	Discharges of high energy	0.6 – 2.5	0.1 -1	> 2
T1	Thermal fault $t < 300^{\circ}\text{C}$	-	-	< 1
T2	Thermal fault $300^{\circ}\text{C} < t < 700^{\circ}\text{C}$	< 0.1	> 1	1 - 4
T3	Thermal fault $t > 700^{\circ}\text{C}$	< 0.2	> 1	> 4

To assist users in diagnosing transformer faults, the MATLAB-based DGA-TRAFADI program was developed using the Rogers ratio method. Its interface is shown in Figure 12b. The input parameters of the DGA - TRAFADI program are the concentrations of the measured gases, including: H<sub>2</sub>, CH<sub>4</sub>, C<sub>2</sub>H<sub>6</sub>, C<sub>2</sub>H<sub>4</sub>, C<sub>2</sub>H<sub>2</sub>, CO<sub>2</sub>, and CO. The output data are the result of diagnosing potential faults in the PT.

The interface of the DGA–TRAFADI program illustrates its readiness for practical use. It simplifies the diagnostic process for testing engineers, enabling them to apply the DGA method quickly and effectively in real operating conditions. This highlights the applied contribution of the study beyond theoretical analysis. The results of diagnosing potential faults in the T1 20 MVA, 110/22 kV transformer using the DGA-TRAFADI software, compared with the diagnostic results from the Southern Vietnam Power Testing Company (EVNSPC), are presented in Table 12.

**Table 12.** Conclusion of Diagnosis of T1 20 MVA, 110/22 kV Transformer Condition Using the DGA Method.

Gas Concentration	DGA-TRAFADI	EVNSPC
H2: 0.00	Thermal fault below 300°C	Thermal fault below 300°C
CH4: 40.43	-	-
C2H6: 18.24	-	-
C2H4: 20.92	-	-
C2H2: 0.00	-	-
CO: 2031.18	-	-
CO2: 8932.66	-	-

Similarly, the results of determining gas concentrations and diagnosing potential faults in the T2 63 MVA, 220 kV transformer using the DGA-TRAFADI software, compared with the diagnostic results from the Southern Vietnam Power Testing Company (EVNSPC), are presented in Table 13.

**Table 13.** Conclusion of Diagnosis of T2 63 MVA, 220 kV Transformer Condition Using the DGA Method.

Gas Concentration	DGA-TRAFADI	EVNSPC
H <sub>2</sub> : 5.124	Slight increase in combustible gases	Slight increase in combustible gases
CH <sub>4</sub> : 6.587	-	-
C <sub>2</sub> H <sub>6</sub> : 0.00	-	-
C <sub>2</sub> H <sub>4</sub> : 3.041	-	-
C <sub>2</sub> H <sub>2</sub> : 3.531	-	-
CO: 7.635	-	-
CO <sub>2</sub> : 2.286	-	-

After diagnosing transformer faults using SFRA and DGA, any detected issues are repaired according to industry standard 623ĐVN/KTNĐ of the Vietnam Electricity Corporation, followed by re-examination to ensure safe operation. These diagnostic methods have been successfully applied at the Southern Vietnam Power Testing Company (EVNSPC).

This paper presents both methods to propose a comprehensive solution covering all transformer fault types: DGA for thermal and electrical faults through dissolved gas analysis, and SFRA for mechanical faults. Although methodological novelty is limited, the study shows how established diagnostic techniques ( $R_{xy}$  for SFRA and Roger ratio for DGA) can be successfully applied in practice, while more advanced approaches have recently been reported in the literature [34], [35].

#### 4. Conclusions

This study demonstrates the combined application of Sweep Frequency Response Analysis (SFRA) and Dissolved Gas Analysis (DGA) for diagnosing power transformer faults. The SFRA–TRAFADI tool effectively identifies mechanical issues in transformer windings, while the DGA–TRAFADI tool diagnoses electrical and thermal faults through gas concentration analysis. Both tools have been implemented and validated with data from the Southern Vietnam Power Testing Company (EVNSPC), thereby demonstrating the practical significance of the research for power utilities in Vietnam.

The main contribution of this work lies in its practical implementation in Vietnam, where reliable transformer operation is critical to power system stability. By integrating these methods into user-friendly MATLAB-based programs, the approach enhances accuracy, supports timely maintenance decisions, and contributes to ensuring a secure and continuous electricity supply.

Future research will explore integrating SFRA and DGA outcomes with advanced approaches such as regression analysis, sliding-window techniques, and AI/ANN-based models to further improve diagnostic reliability and address data limitations.

#### Acknowledgments

This research was supported by the Ho Chi Minh City University of Architecture, Viet Nam

#### Conflict of Interest

The authors declare that they have no known competing financial interests or personal relationships that could have appeared to influence the work reported in this paper.

#### Data Availability Statement

The data used to support the findings of this study are available from the corresponding author upon request.

#### REFERENCES

- [1] A. K. Mehta, R. N. Sharma, S. Chauhan, and S. D. Agnihotri, "Study and diagnosis the failure of power transformer by sweep frequency response analysis," in *Proc. Int. Conf. Power, Energy and Control (ICPEC)*, 2013, doi: 10.1109/ICPEC.2013.6527650.
- [2] T. Mariprasath and V. Kirubakaran. "Power Transformer Faults Identification using SFRA", *International Journal of Scientific & Engineering Research*, vol. 5, no. 5, pp. 81-87, 2014.

- [3] J. B. Dastous and P. Picher, "Transformer and reactor mechanical condition assessment," in *Transformer and Reactor Life Management*, L. Cheim, A. K. Gupta, T. L. MacArthur, and S. Ryder, Eds. Cham: Springer, 2024, pp. 619–664, doi: 10.1007/978-3-031-77219-1\_21.
- [4] G. U. Nnachi and D. V. Nicolae, "Diagnostic methods of frequency response analysis for power transformer winding: A review," in *Proc. IEEE Int. Power Electron. Motion Control Conf. (PEMCC)*, 2016, doi: 10.1109/EPEPEMCC.2016.7752057.
- [5] S. Arumugam, "Theoretical considerations while applying sweep frequency response analysis method in determining the interwinding capacitance of power transformers at higher frequencies," *Eng. Rep.*, 2019, doi: 10.1002/eng2.12036.
- [6] M. A. Habibi *et al.*, "The study of sweep frequency response analysis for inspecting the performance of transformer," in *Proc. Int. Conf. Renewable Energy (ICORE)*, 2019, doi: 10.1088/1742-6596/1595/1/012016.
- [7] S. Wang *et al.*, "An experimental study of the sweep frequency impedance method on the winding deformation of an onsite power transformer," *Energies*, vol. 13, no. 14, p. 3511, Jul. 2020, doi: 10.3390/en13143511.
- [8] O. E. Gouda and S. H. El-Hoshy, "Diagnostic technique for analysing the internal faults within power transformers based on sweep frequency response using adjusted R-square methodology," *IET Science, Measurement & Technology*, vol. 14, no. 10, pp. 1057–1068, Dec. 2020, doi: 10.1049/iet-smt.2020.0048.
- [9] K. V. S. N. Swamy and U. Savadamuthu, "Sweep frequency response-based statistical approach for locating faults in transformer windings using sliding window technique," *Electr. Power Syst. Res.*, vol. 194, p. 107061, 2021, doi: 10.1016/j.epsr.2021.107061.
- [10] Sriyono, U. Khayam, and Suwarno, "SFRA characteristics of power transformer internal winding considering the resonant effect," in *Proc. 8th Int. Conf. Condition Monitoring and Diagnosis (CMD)*, 2020, doi: 10.1109/CMD48350.2020.9287194.
- [11] A. Prasetyo and E. Supriyanto, "Failure analysis of power transformer based on transformer turn ratio test and SFRA," *J. Phys.: Conf. Ser.*, vol. 1837, no. 1, 2021, doi: 10.1088/1742-6596/1817/1/012021.
- [12] S. E. H. Kakolaki, V. Hakimian, J. Sadeh, and E. Rakhshani, "Comprehensive study on transformer fault detection via frequency response analysis," *IEEE Access*, vol. 11, pp. 81852–81881, 2023, doi: 10.1109/ACCESS.2023.3300378.
- [13] Y. Yoon *et al.*, "High-frequency modeling of a three-winding power transformer using sweep frequency response analysis," *Energies*, vol. 14, no. 13, p. 4009, 2021, doi: 10.3390/en14134009.
- [14] B. A. Thango, A. F. Nnachi, G. A. Dlamini, and P. N. Bokoro, "A novel approach to assess power transformer winding conditions using regression analysis and frequency response measurements," *Energies*, vol. 15, no. 7, p. 2335, 2022, doi: 10.3390/en15072335.
- [15] M. M. F. Darwish *et al.*, "Impact of on-grid photovoltaic system on thermal performance of oil-filled transformers," in *Proc. 23rd Int. Middle East Power Syst. Conf. (MEPCON)*, Cairo, Egypt, 2022, pp. 1–5, doi: 10.1109/MEPCON55441.2022.10021729.
- [16] K. V. S. N. Swamy and U. Savadamuthu, "Sweep frequency response-based statistical approach for locating faults in transformer windings using sliding window technique," *Electr. Power Syst. Res.*, vol. 194, p. 107061, 2021, doi: 10.1016/j.epsr.2021.107061.
- [17] M. F. Mohd Yousof, S. Al-Ameri, H. Ahmad, H. A. Illias, and S. N. M. Arshad, "A new approach for estimating insulation condition of field transformers using FRA," *Adv. Electr. Comput. Eng.*, vol. 20, no. 1, pp. 35–42, 2020, doi: 10.4316/AECE.2020.01005.
- [18] S. M. Al-Ameri *et al.*, "The effect of tap changer coking and pitting on frequency response analysis measurement of transformer," in *Proc. IEEE Int. Conf. Properties and Applications of Dielectric Materials (ICPADM)*, Johor Bahru, Malaysia, 2021, pp. 21–24, doi: 10.1109/ICPADM49635.2021.9493956.
- [19] S. Hassan *et al.*, "Partial discharge detection inside transformer oils using on-line monitoring nanotechnology techniques," in *Proc. 20th Int. Middle East Power Syst. Conf. (MEPCON)*, Cairo, Egypt, 2018, pp. 452–454, doi: 10.1109/MEPCON.2018.8635149.
- [20] N. A. Bakar, "High voltage power transformer dissolved gas analysis, measurement and interpretation techniques," in *High Voltage Maintenance Forum – IDC Technologies*, pp. 1-17, 2013.
- [21] H. C. Sun, Y. C. Huang, and C. M. Huang, "A review of dissolved gas analysis in power transformers," *Energy Procedia*, vol. 14, pp. 1220–1225, 2012, doi: 10.1016/j.egypro.2011.12.1079.
- [22] X. F. Wang, Z. D. Wang, Q. Liu, and P. Dyer, "Dissolved gas analysis of thermal faults in transformer liquids simulated using immersed heating method," *IEEE Trans. Dielectr. Electr. Insul.*, vol. 25, no. 5, pp. 1749 - 1757, 2018, doi: 10.1109/TDEI.2018.007158.
- [23] S. A. Ward *et al.*, "Towards precise interpretation of oil transformers via novel combined techniques based on DGA and partial discharge sensors," *Sensors*, vol. 21, no. 6, p. 2223, Mar. 2021, doi:10.3390/s21062223.
- [24] M. K. Patel and A. M. Patel, "Simulation and analysis of DGA for power transformer using advanced control methods," *Asian J. Conver. Technol.*, vol. 7, no. 1, 2021, doi: 10.33130/AJCT.2021v07i01.022, 2021.
- [25] A. M. Aciu, C. I. Nicola, M. Nicola, and M. C. Nițu, "Complementary analysis for DGA based on Duval methods and furan compounds using artificial neural networks," *Energies*, vol. 14, no. 3, p. 588, Jan. 2021, doi:10.3390/en14030588
- [26] H. Cui, L. Yang, Y. Zhu, S. Li, A. Abu-Siada, and S. Islam, "Dissolved gas analysis for power transformers within distributed renewable generation-based systems," *IEEE Trans. Dielectr. Electr. Insul.*, vol. 28, no. 4, pp. 1349 - 1356, Aug. 2021, doi: 10.1109/TDEI.2021.009490.
- [27] S. Y. Petrova, "Practical experience in condition diagnosis gained from oil-immersed power transformers voltage class 10 kV," in *Proc. MMPAM*, 2021, doi: 10.1088/1742-6596/2052/1/012033.
- [28] S. A. Ward, A. El-Faraskoury, M. Badawi, and S. A. Ibrahim, "A modified dissolved gas analysis technique as a diagnostic tool for faults in power transformers," in *Proc. 21st Int. Middle East Power Syst. Conf. (MEPCON)*, Cairo, Egypt, 2019, pp. 639–644, doi: 10.1109/MEPCON47431.2019.9008209.
- [29] *IEC 60076-18: Power Transformers – Part 18: Measurement of Frequency Response*, 2012.
- [30] *IEEE Std C57.149: IEEE Guide for the Application and Interpretation of Frequency Response Analysis for Oil-Immersed Transformers*, 2012.
- [31] *DT/T 911: Frequency Response Analysis on Winding Deformation of Power Transformer*, Chinese Standard, 2004.
- [32] *IEEE Std C57.104: IEEE Guide for the Interpretation of Gases Generated in Oil-Immersed Transformers*, 2019.
- [33] *IEC 60599: Mineral Oil-Filled Electrical Equipment in Service – Guidance on the Interpretation of Dissolved and Free Gas Analysis*, 2015.
- [34] M. Bjelić *et al.*, "Machine learning for power transformer SFRA-based fault detection," *Int. J. Electr. Power Energy Syst.*, vol. 159, p. 109157, 2024, doi: 10.1016/j.ijepes.2023.109779.
- [35] S. A. M. Abdelwahab *et al.*, "Transformer fault diagnosis intelligent system based on DGA methods and neural pattern recognition," *Sci. Rep.*, vol. 15, no. 1, 2025, doi: 10.1038/s41598-024-78293-7.

**Hoang Minh Vu Nguyen** received his M.Sc. degree in electrical engineering from Ho Chi Minh City University of Technology, Vietnam. Currently, he is a lecturer in the Faculty Urban Infrastructure Engineering, University of Architecture Ho Chi Minh City. His main areas of research interests are Microgrid, Sustainable Development, Forecasting, Urban Planning.

E-mail: [vu.nguyenhoangminh@uah.edu.vn](mailto:vu.nguyenhoangminh@uah.edu.vn). ORCID:  <https://orcid.org/0000-0002-2200-6791>. Tel (of Author): 0903676968